Aerosol and Air Quality Research, 16: 1044–1054, 2016

ISSN: 1680-8584 print / 2071-1409 online
doi: 10.4209/aaqr.2015.05.0296

Identification of Long-Range Transport Pathways and Potential Sources of PM_{10} in Tibetan Plateau Uplift Area: Case Study of Xining, China in 2014

Yujie Xin[#], Guochen Wang[#], Li Chen[*]

College of Urban and Environmental Science, Tianjin Normal University, Tianjin 300387, China

ABSTRACT

The aim of the study is to identify long-range transport pathways that may have an important influence on PM_{10} levels in plateau uplift area, namely Xining in northwestern China. Cluster analysis was applied to identify the main trajectory groups in horizontal direction and 3D cluster analysis was employed to identify the origins and distributions of major trajectory groups in vertical direction. Potential Source Contribution Function (PSCF) and Concentration-weighted Trajectory (CWT) were applied to identify the major potential source areas (PSA). Based on the temporal and spatial distribution of backward trajectories, four major trajectory pathways were clustered. The results indicated that Xining was easily affected by inland trajectories in four seasons but there were obvious results that different trajectories have dissimilar influences on the mean PM_{10} concentrations. In horizontal direction, the long-range transport pathways were obvious in spring and winter while a few of long-range transport pathways could be found in summer and autumn. Because wind mainly came from north or west in spring and winter and it was very strong, which had a big influence on the transportation of transport pathways while wind in summer and autumn had a small impact on the transportation of transport pathways. In vertical direction, in the 700 hPa barometric altitude (3000 m) above, air masses in winter and spring with long transport pathways were the most important back-trajectories which had a great influence on Xining city. In summer and autumn, Xining was mainly influenced by airflow distributed below 700 hPa barometric altitude. In spring and winter, eastern Xinjiang, border areas between Gansu and Inner Mongolia and southern Tibet in China with the highest Weight Potential Source Contribution Function (WPSCF) and Weight Concentration-weighted Trajectory (WCWT) values were the dominant potential sources, which demonstrated the contribution from sources outside of Xining were significant. In summer and autumn, WPSCF values outside of Xining were no more than 0.5 (most of them were less than 0.3) and WCWT values were almost lower than 100 μg m^{-3} in those two seasons, which suggested that there were no main important PSA in those two seasons. Furthermore, the study also revealed that Tibet in China was one of the potential sources of PM_{10} in Xining.

Keywords: HYSPLIT; Cluster analysis; PSCF; CWT; PM_{10}; Xining.

INTRODUCTION

PM_{10} is a measure of particles in the atmosphere with a diameter of less than or equal to a nominal 10μm. The guidelines of short-term (24-hour) mean value for PM_{10} (50 μg m^{-3}) and long-term (annual mean) value for PM_{10} (20 μg m^{-3}) is frequently exceeded in the urban environment (WHO, 2005). Guidelines in China of the Class II category of the National Ambient Air Quality (NAAQS) Standards for short-term (24-hour) mean PM_{10} have a limiting value of 150 μg m^{-3}. Previous studies have revealed that the health risks associated with short-term exposure to PM_{10} were likely to be different in cities in developed and developing countries, producing an increase in mortality of about 0.5% for each 10 μg m^{-3} increment in the daily concentrations (Katsouyanni *et al.*, 2001; HEI International Oversight Committee, 2004). The long range transport of particulate matter (PM) which could add to local emissions and the contribution of pollutants particles, especially associations between fine airborne PM exposure and adverse human health (Alolayan *et al.*, 2015; Hellack *et al.*, 2015). It is therefore important to determine long range transportation of particulate matter and potential sources.

Mass concentrations of PM_{10} are affected by long-range transport which could be transported to the downwind regions especially areas characterized by low local emissions (Fu *et al.*, 2008; Karaca *et al.*, 2009). Mineral aerosols from the inner part of the Asian continent are transported to the North Pacific and North America through westerlies (Liu *et al.*,

[#] Contributed equally to this work.

[*] Corresponding author.
E-mail address: chennli@eyou.com

1981; Uematsu *et al.*, 1983; Husar *et al.*, 2001). High mineral dust concentrations have been observed frequently in spring over Japan, a phenomenon called Asian dust (Kosa) (KOSA, 1991; Shinji Kanayama *et al.*, 2002).

Models and observation studies on aerosol transport to the Tibetan Plateau (TP) have been introduced in recent years. Zhao *et al.* (2013) used receptor modeling, namely positive matrix factorization (PMF 3.0, developed by the USEPA), and found that long-range transport of mixed aerosols from the Indo-Gangetic Plain along the valley of the Yarlung Tsangpo River had a significant impact on TP. Liu *et al.* (2015) combined the Spectral Radiation-Transport Model for Aerosol Species (SPRINTARS) with a non-hydrostatic regional model (NHM) to investigate the transport of summer dust and anthropogenic aerosols over the TP and the result showed a spatial variation with heavily loaded dust aerosols over the northern slope and anthropogenic aerosols over the southern slope and to the east of the TP.

HYSPLIT was applied to the study mainly because it had been widely used to identify air mass backward trajectories and origins in given starting locations and it has shown a superior potential (Shan *et al.*, 2009; Masoumi *et al.*, 2013; Rolph *et al.*, 2014; Su *et al.*, 2015). Previous study indicated that HYSPLIT have some inaccuracies and uncertainties in the course of simulating the long range transport of aerosols for the model was influenced by meteorological parameters (wind speed and directions) and the vertical mixing coefficients. However this model did a pretty job to identify dispersion and transportation of pollutants (Alama *et al.*, 2011; Su *et al.*, 2015). Some studies have been conducted to explore PM sources and evolution of Lanzhou, Xi'an, Beijing and areas in the Yangtze River Delta in China, northern Australia and cities in Europe using HYSPLIT as the major tool (Makra *et al.*, 2011; Zhao *et al.*, 2011; Eaglesa *et al.*, 2013; Liu *et al.*, 2013; Cao *et al.*, 2014; Wang *et al.*, 2014). Makra *et al.* (2013) confirmed that the long-range transport pathways had a significant influence on PM_{10} concentrations in two European cities using HYSPLIT model. Givehchi *et al.* (2013) identified that the main source for higher PM_{10} levels in Tehran was middle eastern dust. But few studies were focused on the third pole, TP in the past decades. With global climate changes, studies on Tibetan Plateau are becoming more and more popular in recent years. Wang *et al.* (2015) used PSCF to study the transport of PAHs/PM over the Himalaya Mountains and the locations of the important source regions for PAHs/PM in the southeast TP and found concentrations of particulate-PAHs/TSP showed a seasonal variation with higher concentrations in winter-spring and lower concentrations in summer. Xia *et al.* (2011) using ground-based and satellite remote-sensing data together with an extraordinary pollution episode with an aerosol optical depth at 500 nm(s) to reveal the mechanism anthropogenic activities dramatically perturb the background aerosol levels and aerosol optical properties change in such case in TP. Some studies used single backward trajectory to identify the movements of an air parcel in horizontal direction but it can not identify the origins and distributions of backward trajectories in vertical direction. The use of single back-trajectories comprise great uncertainty. However, groups of back-trajectories involve a much more reliable decision on the potential source areas (PSA) (Stohl, 1998; Makra *et al.*, 2011).

Xining, like most other northwestern cities in China, is easily affected by dust storm each year. Inhabitants in Xining were generally exposed to high levels of daily PM_{10} concentrations (Dou *et al.*, 2012) due to the large number of natural sources and the unique geographic characteristics of a city which is located in a valley namely Huangshui in the edge of TP. Xining was surrounded by a high altitude mountain chain on its north and south boundaries, downstream of the prevailing wind.

The main purpose of this study is to analyze the effects of long-range transport pathways and potential sources of PM_{10} in Xining. The objectives of the research include: (1) to identify the major air masses transport pathways in horizontal and vertical directions using cluster analysis; (2) to stimulate the daily mean PM_{10} concentrations in PSA and identify the main source areas using PSCF method and CWT method and (3) to put forward suggestions to tackle air pollution in region-wide and collaborative efforts in Xining, China.

DATA AND METHODS

Study Location and Monitoring Data

The area of interest in this study is located in Xining (101°77'E, 36°62'N, 2260 m above mean sea level) on the northeastern part of the TP in northwest China (Fig. 1). The land slopes downwards gradually from northwest to southeast. The basin is the transition zone from the TP to the Loess Plateau, which is confined by Qilian mountain to the north, Laji mountain to the south, Riyueshan to the west and a small uplifted block to the east. It is the capital of Qinghai, China with a population about 2.21 million in 2014, which covers an area of 7649 km^2 including 380 km^2 of urban settlement and has four districts and three counties. Typically, there are four distinct seasons in Xining with a long winter and a relatively short spring and autumn. The mean annual temperature and precipitation are 5–6°C and 350–500 mm, respectively. Precipitation occurs mainly in summer.

Daily mean PM_{10} concentrations for Xining during the time period from January 1 to December 31, 2014 were obtained from the National Urban Air Quality Real-time Publishing Platform (available at http://aqistudy.sinaapp.com/). The daily mean PM_{10} loading in Xining was the highest (910.3 $\mu g\ m^{-3}$) on May 9, 2014 and lowest (15.8 $\mu g\ m^{-3}$) on October 11, 2014 (Fig. 2). The daily mean value of PM_{10} concentrations for the ensemble average of the four seasons is 118.16 $\mu g\ m^{-3}$. The results close to the Class II category of the NAAQS in China for PM_{10} with a limiting value of 150 $\mu g\ m^{-3}$ but far exceed the Class I category of the NAAQS for PM_{10} with a limiting value of 50 μgm^{-3}.

Trajectory Data

In this study, 72-hour back-trajectories arriving at 500m above ground level were calculated every 6h a day (04, 10, 16 and 22UTC) from January 1 to December 31, 2014, using the Web version of the HYSPLIT_4 model and data

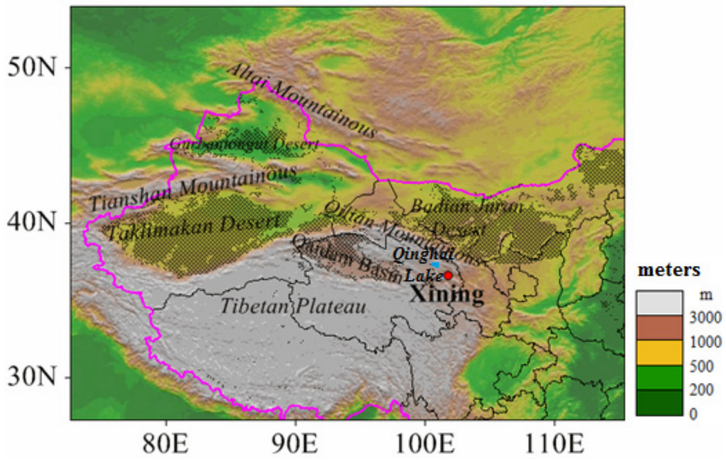

Fig. 1. Topographic map of Xining, China.

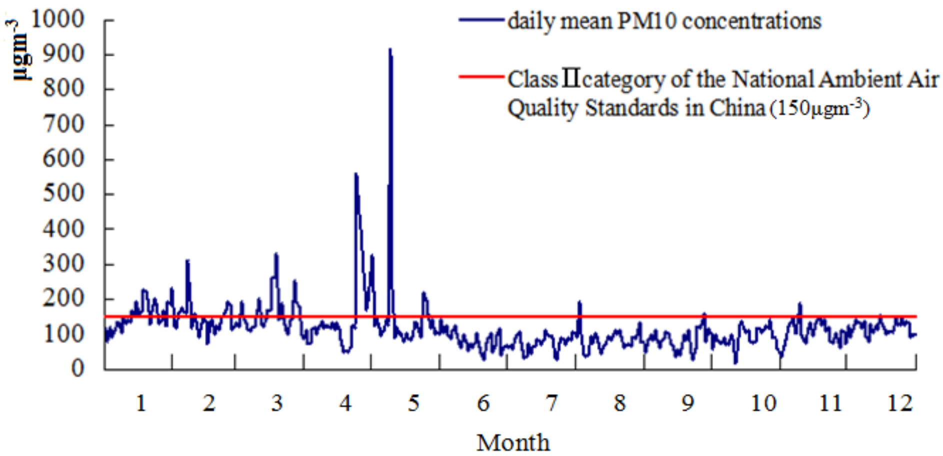

Fig. 2. Daily mean PM_{10} concentrations in Xining, China, 2014.

from NCEP Reanalysis meteorological database (Draxler and Rolph, 2014). Daily meteorological data were obtained from global data assimilation system (GDAS) provided by NECP and it could be downloaded from HYSPLIT website (available at http://www.arl.noaa.gov/ready/hysplit4.html). To represent a well-mixed convective boundary layer for regional transport investigation (Su *et al.*, 2015), the results of our cluster analysis were discussed and presented only for the lowest (h = 500 m) arrival height because back-trajectories at this arrival height have been identified to have the largest influence on the PM concentrations of the target site (McGowan *et al.*, 2008; Hsu *et al.*, 2003a). This height was approximately the height of the mixing layer and has been found to be a generally useful height (Gao *et al.*, 1993).

Trajectory Clustering

Cluster analysis, a multivariate statistical analysis technique, was used as an exploratory tool to divide the trajectory data into distinct transport groups or clusters. TrajStat software has two clustering methods that are Angle distance and Euclidean distance. Euclidean distance is often used to define the latitude and longitude position as variables of the distance between two trajectories. While its main disadvantage is that if two back-trajectories have the same motion path but different speeds, they would be divided into two different categories. To determine the direction from which the air masses reach the site, this study used angle distance, which was defined using the law of cosines (Sirois and Bottenheim, 1995).

$$d_{12} = \frac{1}{n}\sum_{i=1}^{n}\cos^{-1}\left(0.5\frac{\left(A_i + B_i - C_i\right)}{\sqrt{A_i B_i}}\right) \quad (1)$$

$$A_i = \left(X_1(i) - X_0\right)^2 + \left(Y_1(i) - Y_0\right)^2 \quad (2)$$

$$B_i = \left(X_2(i) - X_0\right)^2 + \left(Y_2(i) - Y_0\right)^2 \quad (3)$$

$$C_i = \left(X_2(i) - X_1(i)\right)^2 + \left(Y_2(i) - Y_1(i)\right)^2 \quad (4)$$

where d_{12} is the mean angle between the two backward trajectories, as seen from the trajectory origin point and the variables X_0 and Y_0 define as the position of the receptor site (backward trajectory origin point). X_1 (Y_1) and X_2 (Y_2) reference backward trajectories 1 and 2, respectively.

PSCF Method

PSCF is a calculation to identify the source areas by analyzing trajectory transport pathways (Zeng and Hopke, 1989; Wang *et al.*, 2006; Liu *et al.*, 2013). To analyze possible long-range sources contributing to mean daily PM_{10} concentrations observed in Xining's atmosphere, a single grid cell was calculated by counting each trajectory segment endpoints that terminated within that grid cell. The number of endpoints that fall in *ij*th cell at a time was marked as x_{ij}. While the total number of endpoints that fall in the same grid cell was denoted as y_{ij}. So the PSCF can be defined as

$$PSCF_{ij} = x_{ij}/y_{ij} \tag{5}$$

The PSCF grid covers the study area between the longitudes about 80°–110°E and the latitudes 30°–50°N. Using this method, the study can simulate the PSA that may have an influence on PM_{10} levels in study area. In PSCF analysis, small values of y_{ij} can produce high PSCF values with high uncertainties especially when the number of trajectory pathway or endpoints fall in a grid cell has a short residence time. In order to minimize this artifact, an empirical weight function W_{ij} originally proposed by Zeng and Hopke (1989) was applied when the number of the endpoints in a particular cell was less than about three times the average values of the endpoints per cell (Wang *et al.*, 2006; Xu *et al.*, 2010). That is, WPSCF = W_{ij} × PSCF. So this study defines W_{ij} as flows by referencing previous work:

$$W_{ij} = \begin{cases} 1.00 & 40 < y_{ij} \\ 0.70 & 10 < y_{ij} \le 40 \\ 0.42 & 5 < y_{ij} \le 10 \\ 0.17 & y_{ij} \le 5 \end{cases} \tag{6}$$

CWT Method

A limitation of the PSCF method is that grid cells could have the same PSCF value when sample concentrations were either only slightly higher or much higher than the criterion. As a result, it could be difficult to distinguish moderate sources from strong ones. To identify the sources in each grid, our study applied concentration-weighted trajectory method (CWT). CWT was a way to calculate the concentration weight (Hsu *et al.*, 2003; Wang *et al.*, 2006, 2009; Liu *et al.*, 2013). Using this method, the study can evaluate the value of concentrations weight of PSA which had an effect on the concentrations of PM_{10} levels at Xining. To minimize the inaccuracy caused by the small number of polluted trajectories, arbitrary weight functions are needed to reduce uncertainty and an empirical weight functions W_{ij} in PSCF also can be used in CWT method. The WCWT was defined as WCWT = $W_{ij} \times C_{ij}$. That is,

$$C_{ij} = \frac{k}{\sum_{k=1}^{M} \tau_{ijk}} \sum_{k=1}^{M} C_k \tau_{ijk} \tag{7}$$

where C_{ij} is the average weighted concentration in the *ijth* cell, *k* is the index of the trajectory, *M* is the total number of trajectories, C_k is the concentrations observed on arrival of trajectory *k* and τ_{ijk} is the time spent in the *ij*th cell by trajectory *k*. A high value for C_{ij} implies that air parcels traveling over the *ij*th cell would be, on average, associated with high concentrations at the receptor.

RESULTS AND DISCUSSIONS

Transport Pathways

Long-distance transport pathways of PM_{10} mainly depend on the advection movement in atmosphere (Jing *et al.*, 2008). The dust was transported to downstream areas along airflow that lead to dust-storm weather (Wang *et al.*, 2008). Four main trajectory clusters were divided according to the coherence of the characteristics of spatial distribution of each trajectory using HYSPLIT model. Cluster-mean back-trajectories results for Xining, 2014 were shown in Fig. 3. The number of trajectories assigned to each cluster and daily mean PM_{10} concentrations for each cluster were presented in Table 1. The percentage of polluted trajectories denotes the ratio between the number of polluted trajectories (trajectories cohering with PM_{10} of higher than or equal to the Class II category of the NAAQS (China) for PM_{10} with a limiting value of 150 µg m^{-3}) and the number of all trajectories.

It was found that air masses 1, accounting for about 43.5% of all trajectories started from southeastern Xinjiang province and went through the desert in border areas between Xinjiang and Qinghai province and finally reached Xining in spring. Influenced by northeast airflow in northern Asia, air masses 2, accounting for about 26.4%, made an elliptical movement and passed through cities which were regarded as industrially developed regions of Gansu province and finally moved toward to Xining. The value of daily mean PM_{10} concentrations and polluted trajectories cohering with those two clusters were the highest among the four clusters, 159.5 and 161.4 µg m^{-3}, 12.9% and 7.9%, respectively. Compared with air masses 1, 2 and 4, air masses associated with cluster 3 were less important trajectories. Among those four clusters, clusters 1, 2 and 4 could be regarded as the major polluted trajectories contributing to PM_{10} at Xining and their daily mean PM_{10} concentrations even far exceeded the Class II category of the NAAQS in China (150 µg m^{-3}). In summer, trajectories from inland had a small impact on daily mean PM_{10} levels in Xining. The values of PM_{10} concentrations in Xining linked to the four clusters were very small, and the highest mean PM_{10} concentrations was only 90.9 µg m^{-3}. In autumn, the air masses associated with Cluster 1, accounting for about 59.3%, passed through Taklimakan desert in Tarim basin, Xinjiang Province, then through the southwestern desert in Qaidam basin, Qinghai province and finally toward to Xining, which could be considered as major pollutant trajectories. The air masses associated with Cluster 4, accounting for about 8.7%, had the highest mean PM_{10} concentrations (108.9 µg m^{-3}). The air masses associated with Cluster 2 and 3 were considered less important as pathways for pollutants mainly from northeastern Qinghai province and Hexi Corridor, Gansu province onward to Xining. In winter, air masses associated with cluster 3 and 4, accounting for about 83.9% of all trajectories, could be

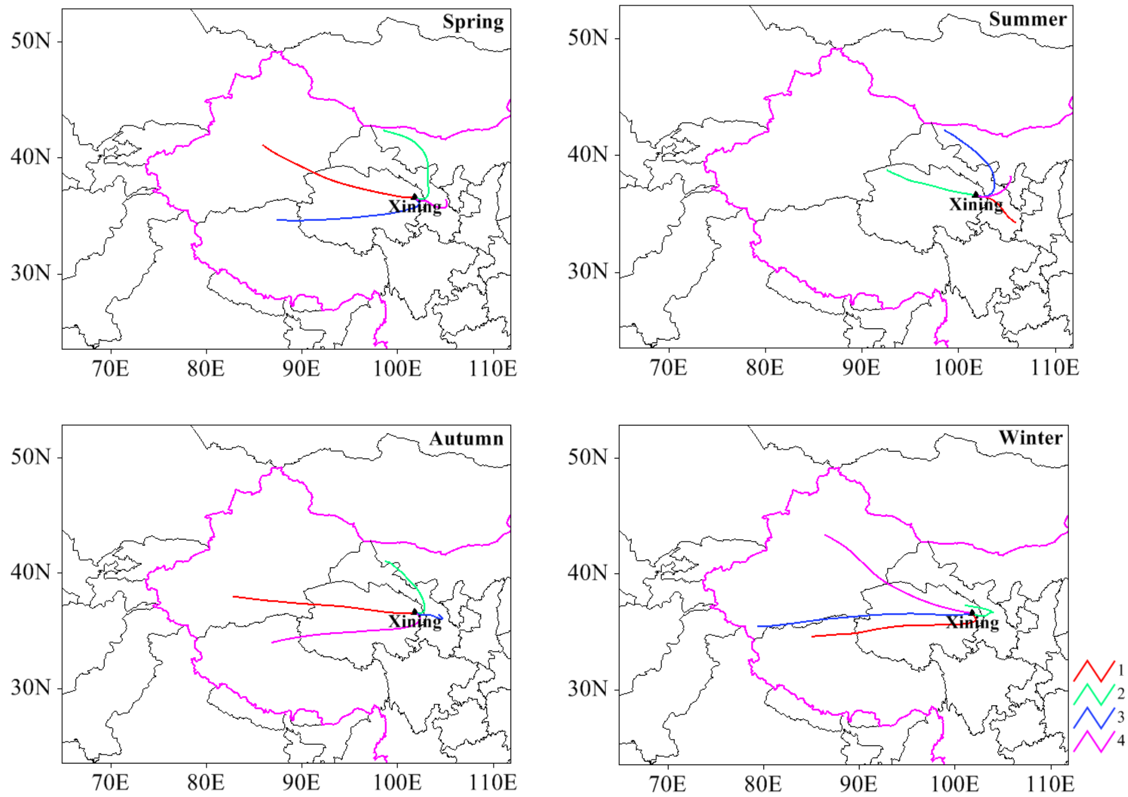

Fig. 3. Cluster-mean back trajectories results for Xining, 2014 using a final cluster number of 4.

Table 1. Percentage of Trajectory Number and Mean PM_{10} Concentrations of Each Cluster in Xining, 2014.

Clusters	Percentage of All Trajectories				Percentage of Polluted Trajectories				Mean PM_{10} Concentrations of All Trajectories (μg m^{-3})			
	Spring	summer	autumn	winter	Spring	summer	autumn	winter	Spring	summer	autumn	winter
1	43.5	30.5	59.3	8.4	12.9	0	1	1.7	159.5	90.9	96.9	133.5
2	26.4	30.8	7.1	7.7	7.9	0	0	3.3	161.4	75.2	61.8	146.3
3	13.7	14.0	24.8	66.5	2.9	1	0	19.3	148.3	86.3	93.2	139.6
4	16.3	24.7	8.7	17.4	4.5	0	1	4.7	155.8	76.6	108.9	138.0

considered as the main air masses which may have a significant influence on daily PM_{10} concentrations in Xining. Cluster 3 and 4, meanwhile, with the greatest number of total trajectories and polluted trajectories were the most important clusters. But air masses associated with Cluster 2 were considered as important pathways with the highest daily PM_{10} concentrations (146.3 μg m^{-3}). In addition, there was a few back-trajectories that can not be divided into any categories which had been classified. So the sum values of percentage of polluted trajectories are less than 1.

Generally speaking, Xining is easily affected by inland trajectories from west and north in the four seasons but there were obvious results that different trajectories have dissimilar influences on the mean PM_{10} concentrations. In spring and winter, airflow from inland is the most important transport pathway with the greatest number of polluted trajectories and the highest value of mean PM_{10} concentrations. In summer and autumn, the air is so clear that these seasons have less important pathways for pollutants and the mean PM_{10} concentrations at Xining was very low in this period of the year. It can be concluded from Fig. 3, trajectory pathways in each season passed through the dust source areas. Dust from Taklimakan desert in Tarim basin, Kumtag desert in eastern Xinjiang, parts of Qaidam basin and Hexi Corridor in Gansu province were the main PSA.

3D Clusters of Backward Trajectories

Single backward trajectory can identify the movements of an air parcel in horizontal direction but it can not identify the sources and distributions of backward trajectory in vertical direction. To get a comprehensive scientific analysis of the characteristics of backward trajectory arriving in Xining, it is essential to further study the distributions of backward trajectory in vertical direction. As it showed in map (Fig. 4), there were obvious differences on distributions of backward trajectory arriving in Xining in vertical direction using 3D backward trajectory analysis.

In spring, there was a significant difference of airflow path in vertical direction. In 700 hPa barometric altitude (3000 m) above, air masses associated with clusters 2 (550

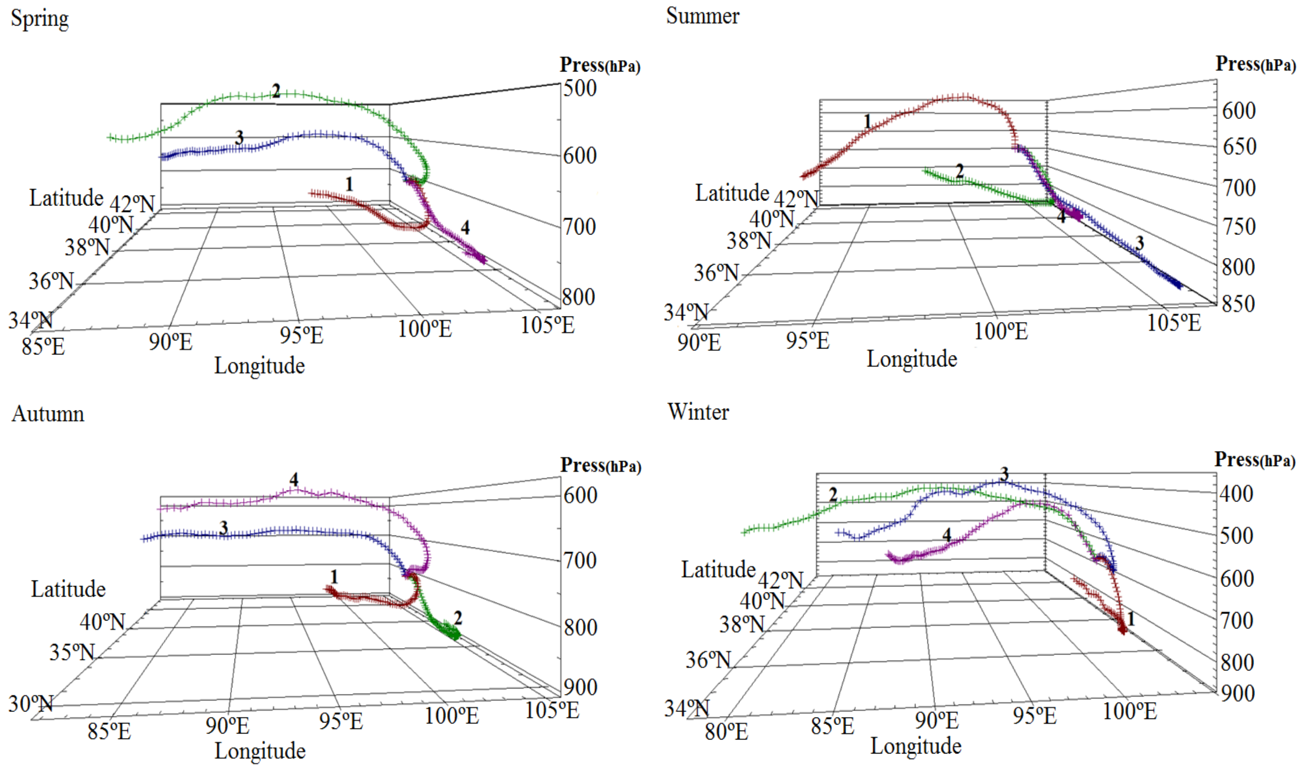

Fig. 4. 3D view of the backward trajectories from Xining, 2014.

hPa) and 3 (690 hPa), with corresponding height of about 5000 m and 3050 m, respectively, were the most important back-trajectories which had a big influence on Xining city. Those clusters had a long transport pathways and passed through the vast inland areas. Blocked by high mountains, those clusters made an arc movement. Those air masses came from the inland northwest passing through Taklamakan desert in Xinjiang and brought desert dust to Xining. In 700 hPa height below, airflow trajectory mainly came from the south and arrived in Xining city. Clusters 1 (750 hPa) and 4 (800 hPa) were corresponding to the height of about 2500 m and 2000 m, respectively. Affected by terrain, cluster 4 passed through industrially developed areas in Lanzhou and carried pollutants to Xining, thus which increased the pollution of Xining city. Cluster 1 mainly passed through the low land areas toward the west upon Xining. In summer, air masses associated with cluster 1 were the most important back-trajectories below 700 hPa barometric altitude. They created an arc movement for these air masses from the northwest inland and they were under the influence of western wind. Blocked by high mountains, those airflow made an arc movement after lifting, carrying dust (natural) along the way to Xining. Cluster 3 and 4 could be regarded as the major polluted trajectories contributing to PM_{10} at Xining below 700 hPa height, and the average barometric altitude is about 800h Pa and 850 hPa with corresponding height of about 2500 m and 1500 m, respectively. Those clusters passed through industrially developed areas in Lanzhou, affected by terrain, climbing along the plateau uplift and carrying anthropogenic contaminants to Xining. In autumn, the air masses associated with clusters 3 (650 hPa) and 4 (600 hPa) corresponding to the height of about 4000 m and 4500 m, respectively, passed through Taklimakan desert in Tarim basin, Xinjiang province, then through the southwestern desert in Qaidam basin, Qinghai province. Blocked by high mountains, those two air masses made an arc movement after lifting and carried dust (natural) along the way to Xining. Cluster 1 and 2, below 700 hPa height with corresponding to the height of about 2000 m, were considered as less important pathways because pollutants are mainly from Northeastern Qinghai province and Hexi Corridor, Gansu province onward to Xining. In winter, air masses associated with clusters 3 and 4 were considered as the most important back-trajectories below 700 hPa barometric altitude. The trajectory of the barometric altitude on average is about 650 hPa (4000 m). Those clusters had long transport pathways and passed through the vast inland areas. Blocked by high mountains, airflow made an arc movement after lifting, carrying dust to Xining city. Compared with cluster 3 and 4, cluster 1 and 2 could be regarded as less important trajectories. Influenced by terrain, those two trajectories carrying anthropogenic contaminants passed through industrially developed areas in Lanzhou and climbed the plateau uplift toward to Xining.

Overall, in winter and spring, Xining was mainly influenced by airflow in 700 hPa barometric altitude above, which had long transport pathways passing through the vast inland areas. What's more, air masses came from eastern Xinjiang, border areas between Gansu and Inner Mongolia and northern Tibet in China. In summer and autumn, Xining was mainly influenced by airflow which was distributed below 700 hPa barometric altitude. Those airflow had short transport pathways passing through the anthropogenic pollutants areas such as Hexi Corridor and Lanzhou, Gansu province.

PSCF Analyses

Cluster analysis provide a useful tool for studying transport pathways of pollutants and identifying the potential transport source areas to Xining. But it has some parameters which were regarded as subjective such as the selections of the clustering algorithm, number of clusters and the distance definition (Wang, 2009). What's more, it can not stimulate the values of daily PM_{10} levels caused by PSA. To get a better understanding of long-range transport that may have an important influence on PM_{10} levels in Xining and to find PSA, further study was needed to analyze the potential sources by using PSCF and CWT methods.

Fig. 5 showed the map for Xining PM_{10} in spring, summer, autumn and winter, 2014 using PSCF method. The colors represent the contribution levels of PSA and the red color could be associated with high concentrations while the blue color represents low PM_{10} concentrations. The map showing the results of the PSCF analysis (Fig. 5), and it could be seen that high WPSCF values were found in Mongolia, desert and semi-desert in border areas between Mongolia and Inner Mongolia, desert and semi-desert regions in Turpan basin, Xinjiang province, Tibetan plateau, Ningxia and Qaidam basin, Qinghai province. Therefore those places could be considered as the main PSA in spring and winter. In summer and autumn, the highest WPSCF values outside of Xining were almost no more than 0.5 and most of them were less than 0.3, which indicated that there were no important PSA in those two seasons. Tibet in China was one of the potential sources of PM_{10} in Xining especially in spring and winter.

CWT Analyses

The results for PM_{10} concentrations identified by CWT method in Fig. 6 were very similar to the results analyzed by PSCF method. The regions with red color, were corresponded to the main contribution sources associated with the highest PM_{10} values (far exceeding 150 µg m^{-3}). In spring, the highest WCWT values covering the map were distributed in Taklimakan desert in Tarim basin, Xinjiang province, Inner Mongolia and central Mongolia. Those areas were the main contribution sources associated with the highest PM_{10} concentrations of 300 µg m^{-3} and parts of Mongolia were even higher than 600 µg m^{-3}, which demonstrated that the contribution from long-range transport and sources outside of Xining were significant. Thus, those places had an important influence on PM_{10} levels in Xining. In summer and autumn, the highest WCWT values outside of Xining were no more than 150 µg m^{-3}, and most of them ranged from 20 to 80 µg m^{-3}, which suggested that there were no main important PSA in those two seasons. In winter, the high WCWT values were mainly located in Taklimakan desert in Tarim basin and Kumtag desert, Xinjiang province, Qaidam basin, Qinghai province and parts of Inner Mongolia with the high WCWT values were about 150–200 µg m^{-3}. Furthermore, contribution from Tibet and Ningxia in four seasons could not be ignored for the region was one of the potential sources of PM_{10} in Xining.

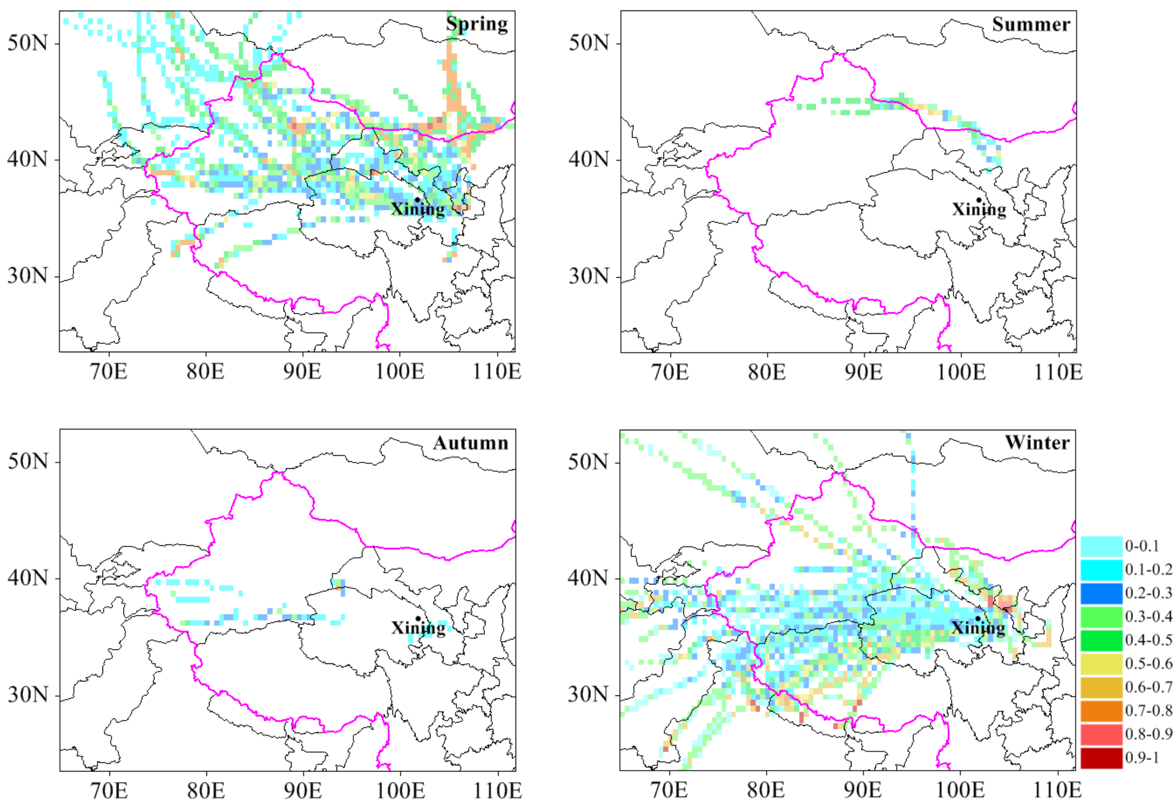

Fig. 5. WPSCF map for Xining PM_{10} in spring, summer, autumn and winter, 2014.

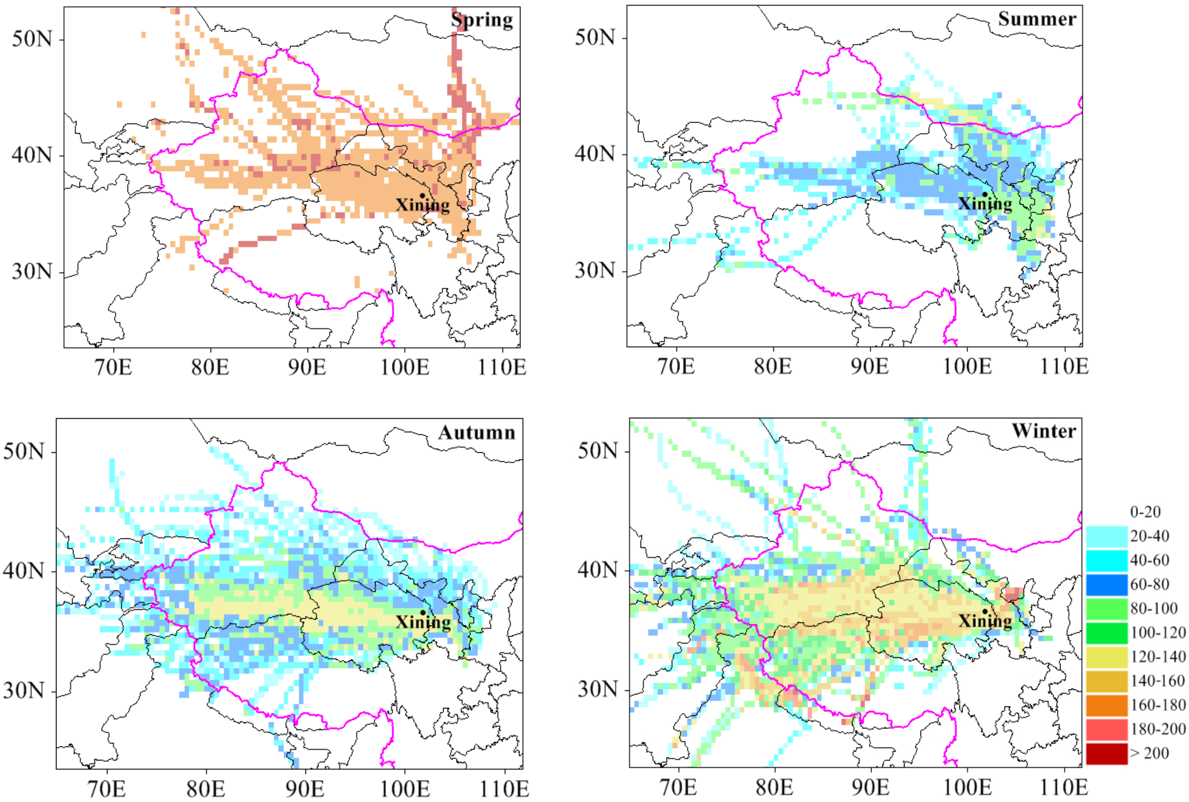

Fig. 6. WCWT map for Xining PM_{10} in spring, summer, autumn and winter, 2014.

There were some uncertainties in the course of using CWT method when the number of trajectory pathways or endpoints fall in a grid cell with short residence time. However, potential areas identified by CWT method have a good coherence with the results determined by using PSCF method. Besides, it would be interesting to associate elemental composition of the measured samples in Xinjiang with those measured in the TaklaMakan Desert (Makra *et al.*, 2002) or possibly from the Lop Desert.

Results of the two methods to identify PSA were not the same. Compared with PSCF, PSA identified by CWT method were more detailed and the contribution of different areas is more easily identified. In winter and spring, CWT method can identify not only the strong PSA with daily mean PM_{10} concentrations in more than 200 µg m^{-3} in Xining city, but also the moderate potential source areas with daily mean PM_{10} concentrations in 150–200 µg m^{-3} which is mainly distributed in the surrounding areas of strong potential areas. Compared with PSCF method, PSA identified by CWT method were broader especially in the summer and autumn. And in this season, the PSA obtained by using PSCF method were mainly distributed in Xinjiang, Inner Mongolia and Gansu in China, where the range is relatively small and dispersed. However, PSA identified by CWT method include not only those results obtained by PSCF method but also some other areas such as parts of Tibet and Ningxia in China. What's more, those areas were not only wide but also concentrated on spatial distribution. So CWT method is more efficient and comprehensive to identify potential source areas than PSCF method.

CONCLUSIONS

To identify the dominant transport pathways at a receptor site, cluster analysis was applied to study backward trajectories arriving at Xining. PSCF and CWT methods were employed to determine the PSA. PSCF method mainly focused on sources identification by using backward trajectory to calculate and describe possible source locations. Compared with PSCF, CWT method could distinguish source strength more easily by assigning the concentrations values at the receptor site to their corresponding trajectories. Four major trajectory pathways in horizontal direction were identified by using trajectory cluster analysis. The trajectory pathways were obvious in spring and winter while a few of trajectory pathways could be found in summer and autumn. Because wind mainly came from north or west in spring and winter and it was very strong, which had a big influence on the transportation of trajectory pathways while wind in summer and autumn had a small impact on the transportation of trajectory pathways. Spring and winter with the greatest number of polluted trajectories, thus had the highest value of mean PM_{10} concentrations. Compared with spring and winter, daily mean PM_{10} concentrations in Xining influenced by trajectory in summer and autumn was less important, thus the value of mean PM_{10} concentrations was very low due to the clear air masses. There were obvious differences on distributions of backward trajectories arriving in Xining in vertical direction using 3D backward trajectory analysis. Back trajectories, below 700 hPa atmosphere level, with long transport pathways which were considered as the most important back trajectories. But back trajectories, above 700 hPa atmosphere level, have short transport pathways which might have an important influence on Xining.

PSCF and CWT methods were applied to identify the PM_{10} levels and PSA. In spring and winter, eastern Xinjiang, border areas between Xinjiang and Mongolia and southern Tibet in China, with the highest WPSCF values and WCWT values were the dominant potential sources, which demonstrated the contribution from sources outside of Xining were significant. In summer and autumn, WPSCF values outside of Xining were no more than 0.5 and most of them were less than 0.3 and WCWT values were almost lower than 150 $\mu g\ m^{-3}$ in those two seasons, which suggested that there were no main important PSA in those two seasons. Furthermore, the study also revealed that Tibet and Ningxia in China were the potential sources of PM_{10} in Xining. Compared with PSCF method, CWT showed a superior potential and it is more efficient and comprehensive to identify PSA.

Through this research, we found that there was a seasonal variations of transport pathways. Spring and winter with the greatest number of polluted trajectories, thus had the highest value of daily mean PM_{10} concentrations. However, in summer and autumn there was no polluted trajectories, thus the value of daily mean PM_{10} concentrations was very low. What's more, we innovatively used 3D backward trajectory analysis and found backward trajectories which might have an important influence on Xining were most distributed below 700 hPa atmosphere level in spring and winter and above 700 hPa atmosphere level in summer and autumn, respectively. Our findings revealed that there was a seasonal and spatial variations of airflow in vertical direction in Xining. Using PSCF and CWT methods, we identified the most important PSA and found daily mean concentrations of PM_{10} showed a seasonal variation with higher concentrations in winter-spring and lower concentrations in summer-autumn. In future study, we will carry out researches for distribution of PSA and air transportation pathways which have lasted for many years combining with an extraordinary case. Our study will improve the accuracy and scientificity of the models we used.

ACKNOWLEDGEMENTS

This work was supported by National Natural Science Funds of China (Grant No. 41205101/D0512). Special thanks to National Urban Air Quality Real-time Publishing Platform for help with daily mean PM_{10} concentrations data. We also gratefully acknowledge the NOAA Air Resources Laboratory (ARL) for the provision of the HYSPLIT model used in this publication.

REFERENCES

Alama, K., Qureshi, S. and Blaschke, T. (2011). Monitoring Spatio-temporal Aerosol Patterns over Pakistan Based on MODIS, TOMS and MISR Satellite Data and a HYSPLIT Model. *Atmos. Environ*. 45: 4641–4651.

Alolayan, M.A., Brown, K.W., Evans, J.S., Bouhamra, W.S. and Koutrakis, P. (2015). Source Apportionment of Fine Particles in Kuwait City. *Sci. Total Environ*. 448: 14–25.

Cao, C.X., Zheng, S. and Singh, R.P. (2014). Characteristics of Aerosol Optical Properties and Meteorological Parameters during Three Major Dust Events (2005-2010) over Beijing, China. *Atmos. Res*. 150: 129–142.

Dou, X.Y., Xu, J. and Han, D.H. (2012). Transportation Characteristics of PM_{10} in the Typical Pollution Weather in Xining. *J. Meteorol. Environ.* 28: 85–90 (in Chinese).

Draxler, R.R. and Rolph, G.D. (2014). HYSPLIT (HYbrid Single-Particle Lagrangian Integrated Trajectory) Model Access via NOAA ARL READY Website (http://ready.arl.noaa. gov/HYSPLIT.php) NOAA Air Resources Laboratory, Silver Spring, MD.

Eaglesa, D., Walkera, P.J., Zaluckib, M.P. and Durra, P.A. (2013). Modelling Spatio-temporal Patterns of Long-distance Culicoides Dispersal into Northern Australia. *Prev. Vet. Med.* 110: 312–322.

Fu, P., Huang, J., Li, C. and Zhong, S. (2008). The Properties of Dust Aerosol and Reducing Tendency of the Dust Storms in Northwest China. *Atmos. Environ*. 42: 5896–5904.

Gao, N., Cheng, M.D. and Hopke, P.K. (1993). Potential Source Contribution Function Analysis and Source Apportionment of Sulfur Species Measured at Rubidoux, CA during the Southern California Air Quality Study, 1987. *Anal. Chim. Acta.* 277: 369–380.

Givehchi, R., Arhami, M. and Tajrishy, M. (2013). Contribution of the Middle Eastern Dust Source Areas to PM_{10} Levels in Urban Receptors: Case Study of Tehran, Iran. *Atmos. Environ*. 75: 287–295.

HEI (2000). Reanalysis of the Harvard Six-Cities Study and the American Cancer Society Study of Particulate Air Pollution and Mortality. A Special Report of the Institute's Particle Epidemiology Reanalysis Project. Cambridge, MA, Health Effects Institute.

Hellack, B., Quass, U., Beuck, H., Wick, G., Kuttler, W., Schins, R.P.F. and Kuhlbusch, T.A.J. (2015). Elemental Composition and Radical Formation Potency of PM_{10} at an Urban Background Station in Germany in Relation to Origin of Air Masses. *Atmos. Environ*. 105: 1–6.

Hsu, Y.K., Holsen, T. and Hopke, P.K. (2003). Comparison of Hybrid Receptor Models to Locate PCB Sources in Chicago. *Atmos. Environ*. 37: 545–562.

Hsu, Y.K., Holsen, T. and Hopke, P.K. (2003a). Locating and Quantifying PCB Sources in Chicago: Receptor Modeling and Field Sampling. *Environ. Sci. Technol.* 37: 681–690.

Husar, R.B., Tratt, D.M., Schichtel, B.A., Falke, S.R., Li, F., Jaffe, D., Gasso, S., Gill, T., Laulainen, N.S., Lu, F., Reheis, M.C., Chun, Y., Westpal, D., Holben, B.N., Gueymard, C., McKendry, I., Kuring, N., Feldman, G.C., McClain, C., Frouin, R.J., Merrill, J., DuBois, D., Vignola, F., Murayama, T., Nickovic, S., Wilson, W.E., Sassen, K., Sugimoto, N. and Malm, W.C. (2001). Asian Dust Events of April 1998. *J. Geophys. Res.* 106: 18317–18330.

Jing, J.S., Fu, G. and Chen, D. (2008). Seasonal Variation

Characteristics of TSP and PM_{10} in Beijing. *Period. Ocean Univ. China* 38: 539–541 (in Chinese).

Karaca, F., Anil, I. and Alagha, O. (2009). Long-range Potential Source Contributions of Episodic Aerosol Events to PM_{10} Profile of a Megacity. *Atmos. Environ*. 43: 5713–5722.

Katsouyanni, K. (2001). Confounding and Effect Modification in the Short-term Effects of Ambient Particles on Total Mortality: Results from 29 European Cities within the APHEA2 Project. *Epidemiology* 12: 521–531.

KOSA (1991). Water Research Institute of Nagoya University (Ed.), KOSA. KOKON Press, Tokyo (in Japanese).

Liu, N., Ye, Y., He, J.J. and Zhao, S.P. (2013). Integrated Modeling of Urban-scale Pollutant Transport: Application in a Semi-arid Urban Valley, Northwestern China. *Atmos. Pollut. Res*. 4: 306–314.

Liu, T., Gu, X., An, Z. and Fan, Y. (1981). The Dust Fall in Beijing, China on April 18, 1980. *Geol. Soc. Am. Special Pap.* 186: 149–157.

Liu, Y., Sato, Y., Jia, R., Xie, Y., Huang, J. and Nakajima, T. (2015). Modeling Study on the Transport of Summer Dust and Anthropogenic Aerosols over the TP. *Atmos. Chem. Phys. Discuss.* 15: 15005–15037.

Makra, L., Borbély-Kiss, I., Koltay, E. and Chen, Y. (2002). Enrichment of Desert Soil Elements in Takla Makan Dust Aerosol. *Nucl. Instrum. Methods Phys. Res., Sect. B* 189: 214–220.

Makra, L., Matyasovszky, I., Guba, Z., Karatzas, K. and Anttila, P. (2011). Monitoring the Long-range Transport Effects on Urban PM_{10} Levels using 3D Clusters of Backward Trajectories. *Atmos. Environ*. 45: 2630–2641.

Makra, L., Ionel, I., Csépe, Z., Matyasovszky, I., Lontis, N., Popescu, F. and Sümeghy, Z. (2013). Characterizing and Evaluating the Role of Different Transport Modes on Urban PM_{10} Levels in Two European Cities Using 3D Clusters of Backward Trajectories. *Sci. Total Environ*. 458–460: 36–46.

Masoumi, A., Khalesifard, H.R., Bayat, A. and Moradhaseli, R. (2013). Retrieval of Aerosol Optical and Physical Properties from Ground-based Measurements for Zanjan, a City in Northwest Iran. *Atmos. Res*. 120–121: 343–355.

McGowan, H. and Clark, A. (2008). Identification of Dust Transport Pathways from Lake Eyre, Australia Using Hysplit. *Atmos. Environ*. 42: 6915–6925.

Rolph, G.D., Ngan, F. and Draxler, R.R. (2014). Modeling the Fallout from Stabilized Nuclear Clouds Using the HYSPLIT Atmospheric Dispersion Model. *J. Environ. Radioact.* 136: 41–55.

Shan, W.P., Yin, Y.Q., Lu, H.X. and Liang, S.X. (2009). A Meteorological Analysis of Ozone Episodes Using HYSPLIT Model and Surface Data. *Atmos. Res.* 93: 767–776.

Shinji, K., Sadayo, Y., Fumitaka, Y. and Remi, M. (2002). The Chemical and Strontium Isotope Composition of Atmospheric aerosols over Japan: The Contribution of Long-range-transported Asian Dust (Kosa). *Atmos. Environ*. 36: 5159–5175.

Sirois, A. and Bottenheim, J.W. (1995). Use of Backward Trajectories to Interpret the 5-year Record of PAN and O_3 Ambient Air Concentrations at Kejimkujik National Park, Nova Scotia. *J. Geophys. Res*. 100: 2867–2881.

Stohl, A. (1998). Computation, Accuracy and Applications of Trajectories–A Review and Bibliography. *Atmos. Environ.* 32: 947–966.

Su, L., Yuan, Z.B., Fung, J.C.H. and Lau, A.K.H. (2015). A Comparison of HYSPLIT Backward Trajectories Generated from Two GDAS Datasets. *Sci. Total Environ*. 506–507: 527–537.

Uematsu, M., Duce, R.A., Prospero, J.M., Chen, L., Merrill, J.T. and McDonald, R.L. (1983). Transport of mineral aerosol from Asia over the North Pacific Ocean. *J. Geophys. Res*. 88: 5343–5352.

Wang, H.L., Zhu, B., Shen, L.J., An, J.L., Yin, Y. and Kang, H.Q. (2014). Number Size Distribution of Aerosols at Mt. Huang and Nanjing in the Yangtze River Delta, China: Effects of Air Masses and Characteristics of New Particle Formation. *Atmos. Res*. 150: 42–56.

Wang, J., Yan, Q. and Wang, H.Z. (2008). Study on an Infrequent Multi-day Air Pollution Episode in Shanghai. *Clim. Environ. Res*. 13: 53–60.

Wang, X.P., Gong, P., Sheng, J.J., Zhao, Z., Joswiak, D.R. and Yao, T.D. (2015). Long-range Atmospheric Transport of Particulate Polycyclic Aromatic Hydrocarbons and the Incursion of Aerosols to the Southeast Tibetan Plateau. *Atmos. Environ*. 115: 124–131.

Wang, Y.Q., Arimoto, R. and Zhang, X.Y. (2006). The Contribution from Distant Dust Sources to the Atmospheric Particulate Matter Loading at Xi'an, China during Spring. *Sci. Total Environ*. 368: 875–883.

Wang, Y.Q., Zhang, X.Y. and Draxler, R. (2009). TrajStat: GIS-based Software that Uses Various Trajectory Statistical Analysis Methods to Identify Potential Sources from Long-term Air Pollution Measurement Data. *Environ. Modell. Software* 24: 938–939.

WHO (World Health Organization) (2005). WHO Air Quality Guidelines for Particulate Matter, Ozone, Nitrogen Dioxide and Sulfur Dioxide (Global Update 2005). Available from: WHO Press, World Health Organization, 20 Avenue Appia, 1211 Geneva 27, Switzerland.

Xia, X.G., Zong, X.M., Cong, Z.Y., Chen, H.B., Kang, S.C. and Wang, P.C. (2011). Baseline Continental Aerosol over the Central Tibetan Plateau and a Case Study of Aerosol Transport from South Asia. *Atmos. Environ*. 45: 7370–7378.

Xu, X. and Akhtar, U.S. (2010). Identification of Potential Regional Sources of Atmospheric Total Gaseous Mercury in Windsor, Ontario, Canada Using Hybrid Receptor Modeling. *Atmos. Chem. Phys*. 10: 7073–7083.

Zeng, Y. and Hopke, P.K. (1989). A Study on the Sources of Acid Precipitation in Ontario, Canada. *Atmos. Environ*. 23: 1499–1509.

Zhao, P., Zhang, X., Xu, X. and Zhao, X. (2011). Long-term Visibility Trends and Characteristics in the Region of Beijing, Tianjin, and Hebei, China. *Atmos. Res*. 101: 711–718.

Zhao, Z.Z., Cao, J.J., Shen, Z.X., Xu, B.Q., Zhu, C.S., Antony, C.L.-W., Su, X.L., Liu, S.X., Han, Y.M., Wang, G.H. and Ho, K.F. (2013). Aerosol Particles at a High-altitude Site on the Southeast Tibetan Plateau, China: Implications for Pollution Transport from South Asia. *J. Geophys. Res.* A118: 11360–11375.

Received for review, May 11, 2015
Revised, July 11, 2015
Accepted, August 23, 2015